CHAPTER 6

Synthesis of Ni-Zn Ferrite nanopowders by using Oxalate precursor based method

6.1 Experimental Procedure for Chemical Synthesis:

The chemicals used were $Fe(NO_3)_3.9H_2O$ (99.9%, Merck, India), $Ni(NO_3)_2.6H_2O$ (99.9%, Merck, India), Zn powder (99.9%, Merck, India), and oxalic acid (99.9%, Merck, India) without further purification. $Zn(NO_3)_2$ was prepared by dissolving Zn dust in aqueous nitric acid.

Stoichiometric amounts of metal nitrates were dissolved in distilled water according to the molar compositions as shown in Table 6.1.

Table 6.1. Molar ratio of starting compounds.

Target Composition	$Fe(NO_3)_3.9H_2O$	$Ni(NO_3)_2.6H_2O$	Zn	Oxalic acid
$Ni_{0.80}Zn_{0.20}Fe_2O_4$	0.084	0.034	0.008	0.01575
$Ni_{0.65}Zn_{0.35}Fe_2O_4$	0.084	0.027	0.015	0.01575
$Ni_{0.50}Zn_{0.50}Fe_2O_4$	0.084	0.021	0.021	0.01575
$Ni_{0.40}Zn_{0.60}Fe_2O_4$	0.084	0.017	0.025	0.01575

Aqueous solutions of metal nitrates and oxalic acid were mixed in a molar ratio of 1:0.125.The solutions were stirred for 1hour at room temperature using a magnetic stirrer. Dark brown precursors were formed when the mixtures were evaporated to dryness on a hot plate at ~125^0C.

The precursor powders were then calcined in air in temperatures ranging from 450 to 850^{0}C for two and a half hours in air to obtain Ni-Zn ferrite nanopowders [136]. In order to avoid contamination of the precursors by carbon, a few drops of saturated ammonium nitrate solution was added to the precursor powders during calcination.

6.2 Results and Discussion:

6.2.1 Thermal Analysis:

TG-DTG and DSC analyses were performed to investigate the decomposition behavior of the precursor powders due to heat treatment in air and thermograms are shown in Fig 6.1(a-d).

The important features of the thermograms are as follows:

(i) In TG thermogram, a total weight loss of ~ 25-50% (depending on the composition) was observed when the sample was heated between 30 to 900^{0}C in air.

(ii) Weight loss of ~10-15% occurred between 30 and 150^{0}C and that was assigned to the removal of hydrated water of oxalate precursor. This weight loss was reflected in DSC thermogram as an endothermic peak in the temperature range of ~75-80^{0}C.

(iii) Major weight loss of ~15-35% occurred in the region from 200 to 550^{0}C and this weight loss was attributed to loss of metal coordinated water molecules as well as to the decomposition of carbonaceous mass of the precursor.

(iv) In DSC thermogram, the exothermic peak for the decomposition of the carbonaceous mass (which was very less in comparison to the metal ions concentration) and the strong endothermic peak due to loss of metal coordinated water molecules lay in the same temperature range (~270-300^{0}C) [136].

(iv) The minor exothermic peak corresponding to the decomposition of the carbonaceous mass was present between 400-420^{0}C for all precursors.

(v) Heating the sample beyond 550^{0}C did not result in a significant weight loss in the samples. The trivial weight loss (~1-2%) beyond this temperature was only due to slow oxidation of carbonaceous material in the precursor.

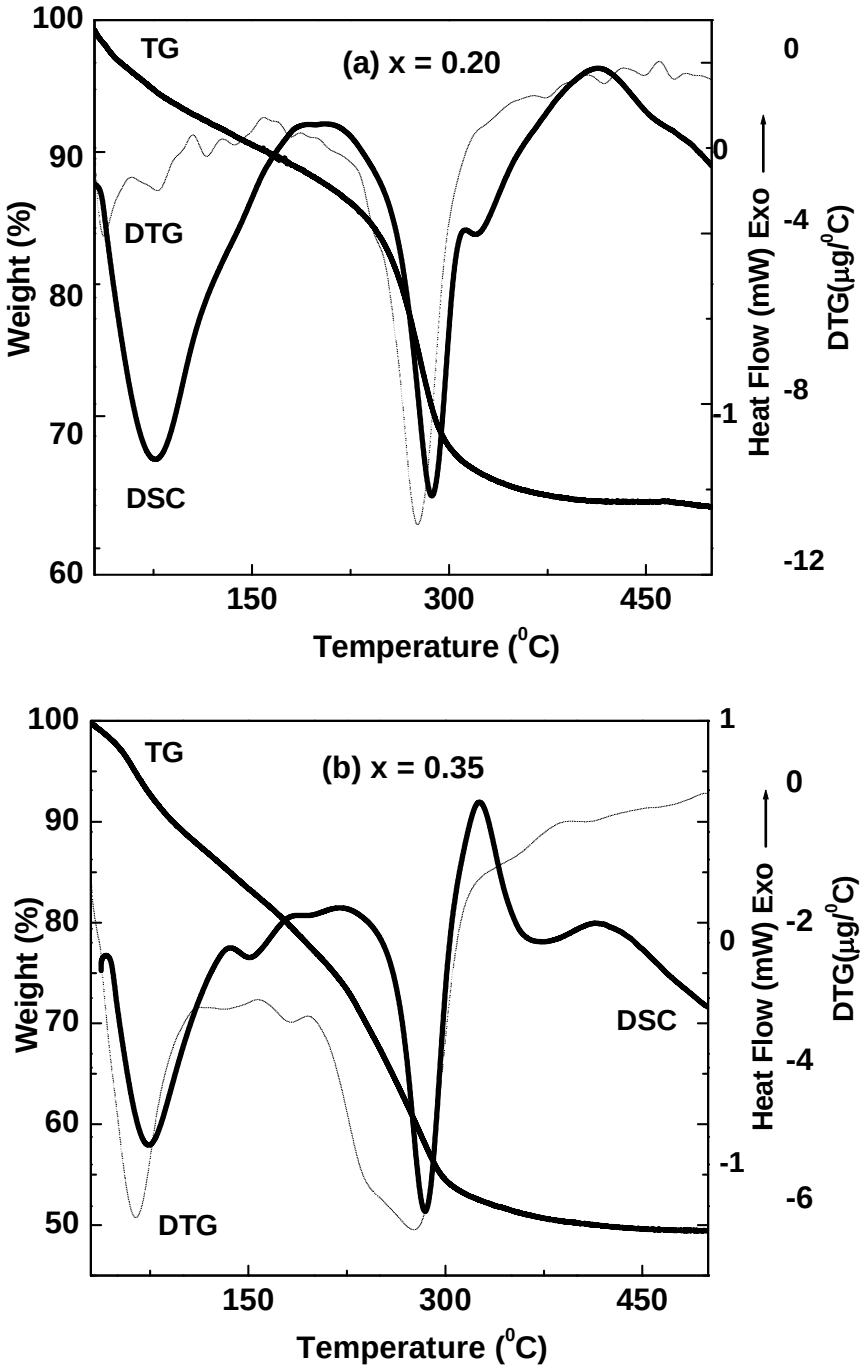

Fig. 6.1 continued

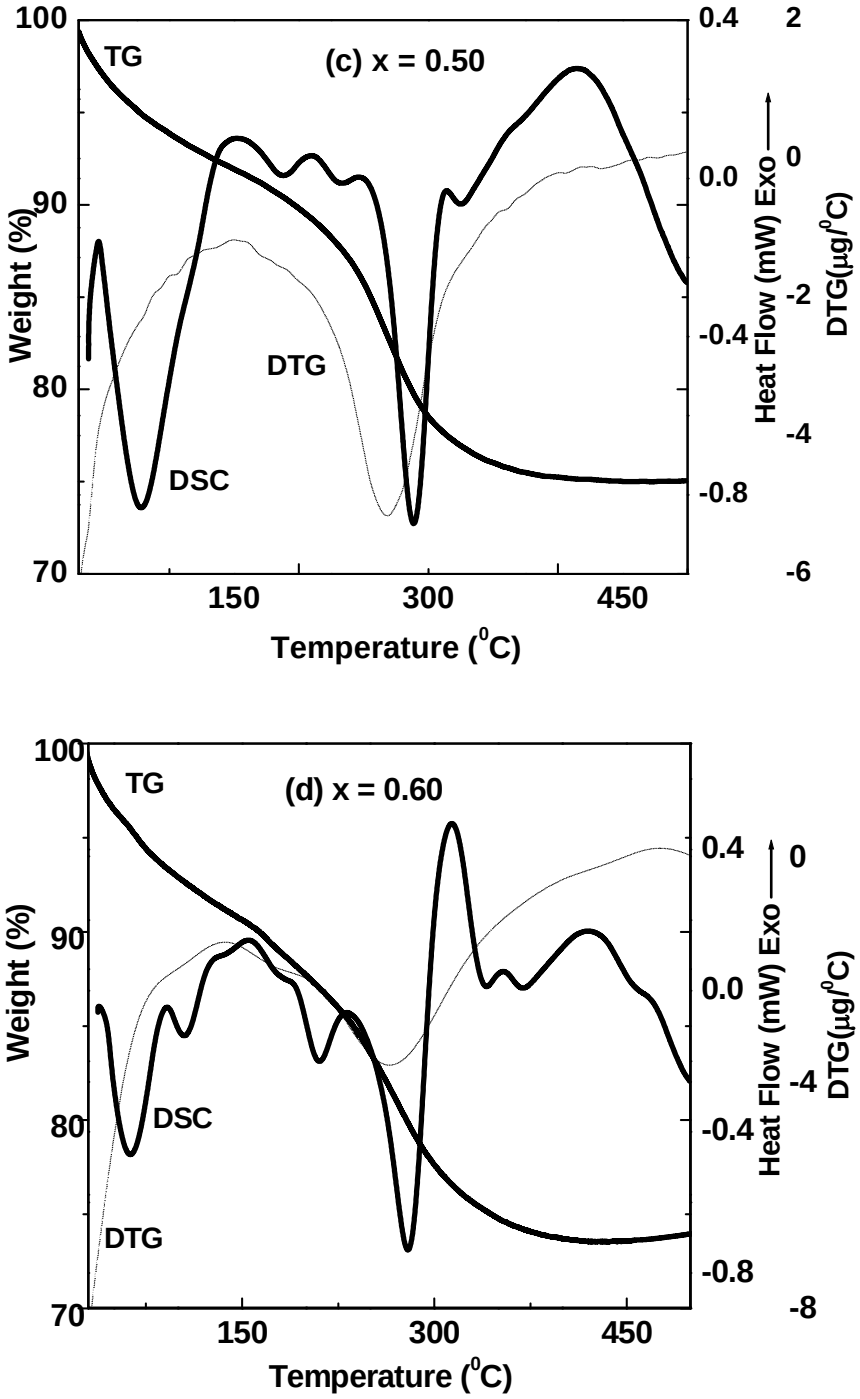

Fig. 6.1 TG-DTG and DSC thermograms for precursor powders of (a) $Ni_{0.80}Zn_{0.20}Fe_2O_4$ and (b) $Ni_{0.65}Zn_{0.35}Fe_2O_4$ i (c) $Ni_{0.50}Zn_{0.50}Fe_2O_4$ and (d) $Ni_{0.40}Zn_{0.60}Fe_2O_4$ in air.

6.2.2 XRD Analysis:

Room temperature XRD spectra of powders at different calcinations temperatures for all values of x are shown in Fig. 6.2 (a-d).

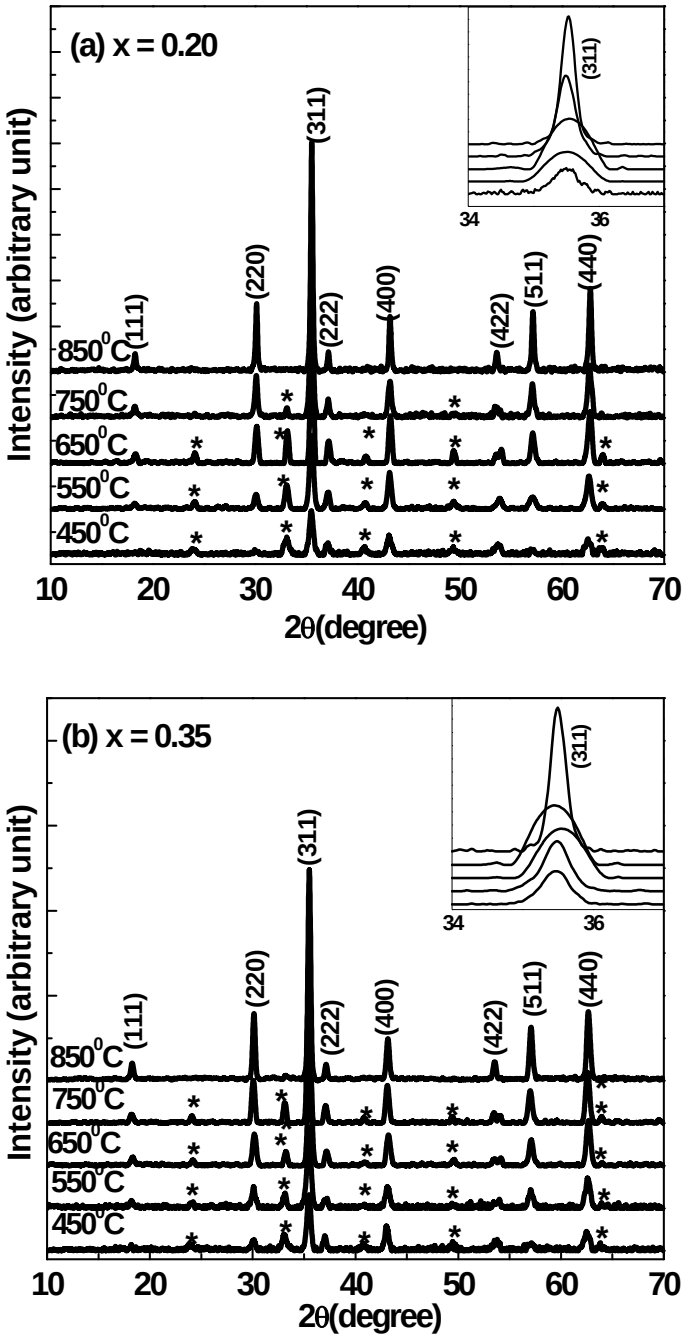

Fig. 6.2 continued

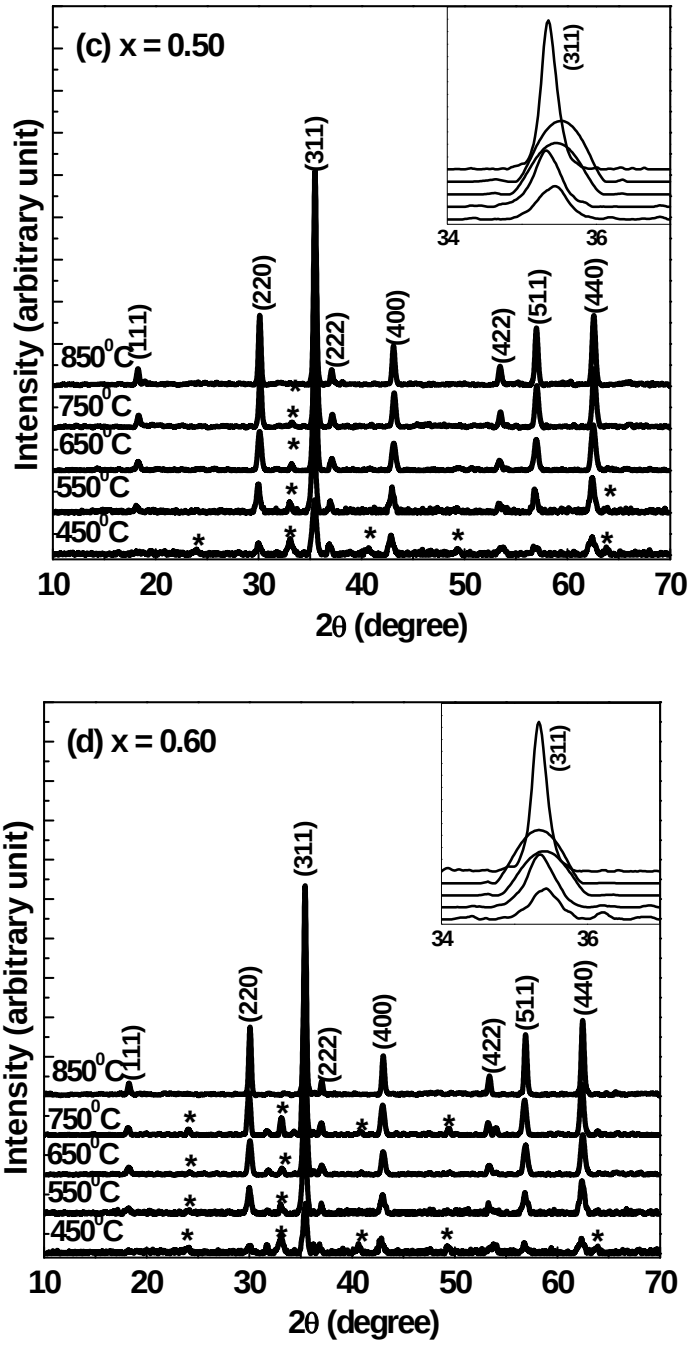

Fig. 6.2 XRD spectra of precursor powders of (a) $Ni_{0.80}Zn_{0.20}Fe_2O_4$ (b) $Ni_{0.65}Zn_{0.35}Fe_2O_4$ (c) $Ni_{0.50}Zn_{0.50}Fe_2O_4$ (d) $Ni_{0.40}Zn_{0.60}Fe_2O_4$ ferrites, at different calcination temperatures. Slow scan of the (311) diffraction plane are shown in the insets. Impurity phase is marked by (*) and corresponds to pure hematite.

The main features of the spectra are as follows:

(i) The appearance of the main intensity peaks corresponding to (311) diffraction planes for powder calcined at 450^0C, indicated the beginning of the formation of Ni-Zn ferrite phase.

(ii) Although Ni-Zn ferrite phase is present for each precursor powder calcined at a different temperature, peaks corresponding to α-Fe_2O_3 (hematite) as an impurity phase were also present. The peaks for impurity phase are marked as (*) and correspond to (012), (104), (113), (024) and (300) diffraction planes of pure hematite (JCPDS 80-2377).

(iii) Complete formation of single-phase Ni-Zn ferrite occurred when precursor was calcined at 850^0C for two and a half hours in air [136]. Peaks corresponding to (111), (220), (311), (222), (400), (422), (511) and (440) diffraction planes of Ni-Zn ferrite were present for the pure phase (JCPDS 08-0234).

(iv)Crystallite size of powders calcined at different temperatures was calculated using Scherrer's equation [125] and they lie in the range of 15-30 nm depending upon the calcination temperature.

6.2.3 TEM Analysis:

TEM micrographs for the powders calcined at 850^0C are shown in Fig. 6.3 (a) and (b). The micrographs clearly indicated that average particle size of the calcined powder was ~35 nm and it matched well with that calculated from XRD data. The particles were mostly spherical in shape and formed loose aggregates.

.

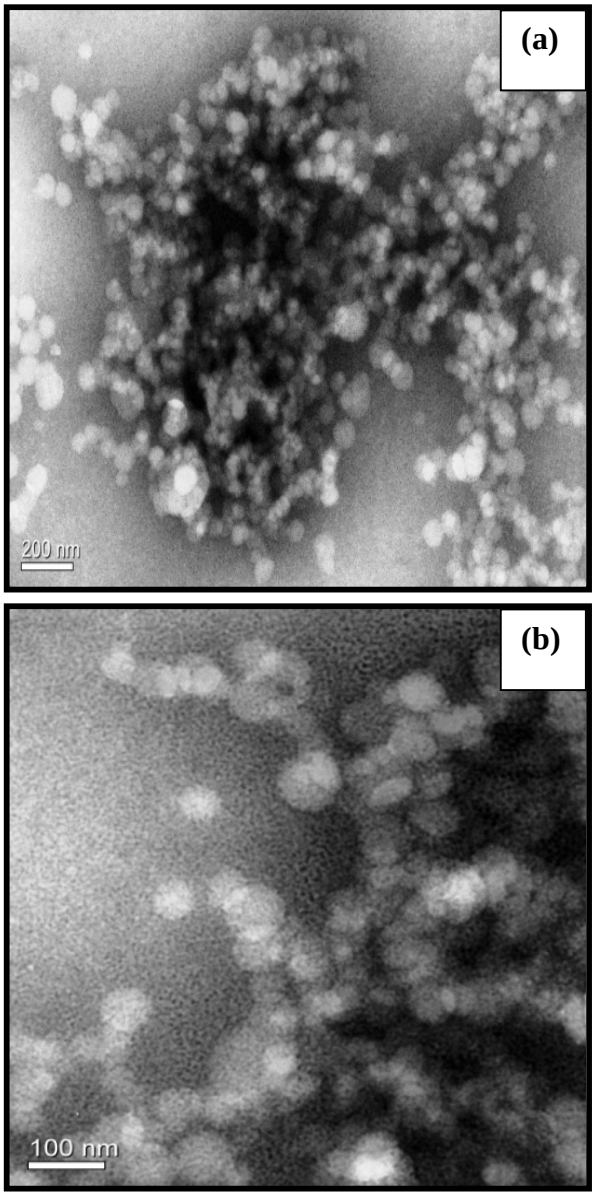

Fig 6.3 TEM micrographs of $Ni_{1-x}Zn_xFe_2O_4$ nanopowders for (a) x = 0.20 and (b) x = 0.60, synthesized at a calcination temperature of 850^0C.

6.2.4 SEM Analysis:

SEM was used to investigate the change of microstructures of the as synthesized $Ni_{1-x}Zn_xFe_2O_4$ nanopowders with change in sintering temperature and composition and these are shown in Fig 6.4 (a-i).

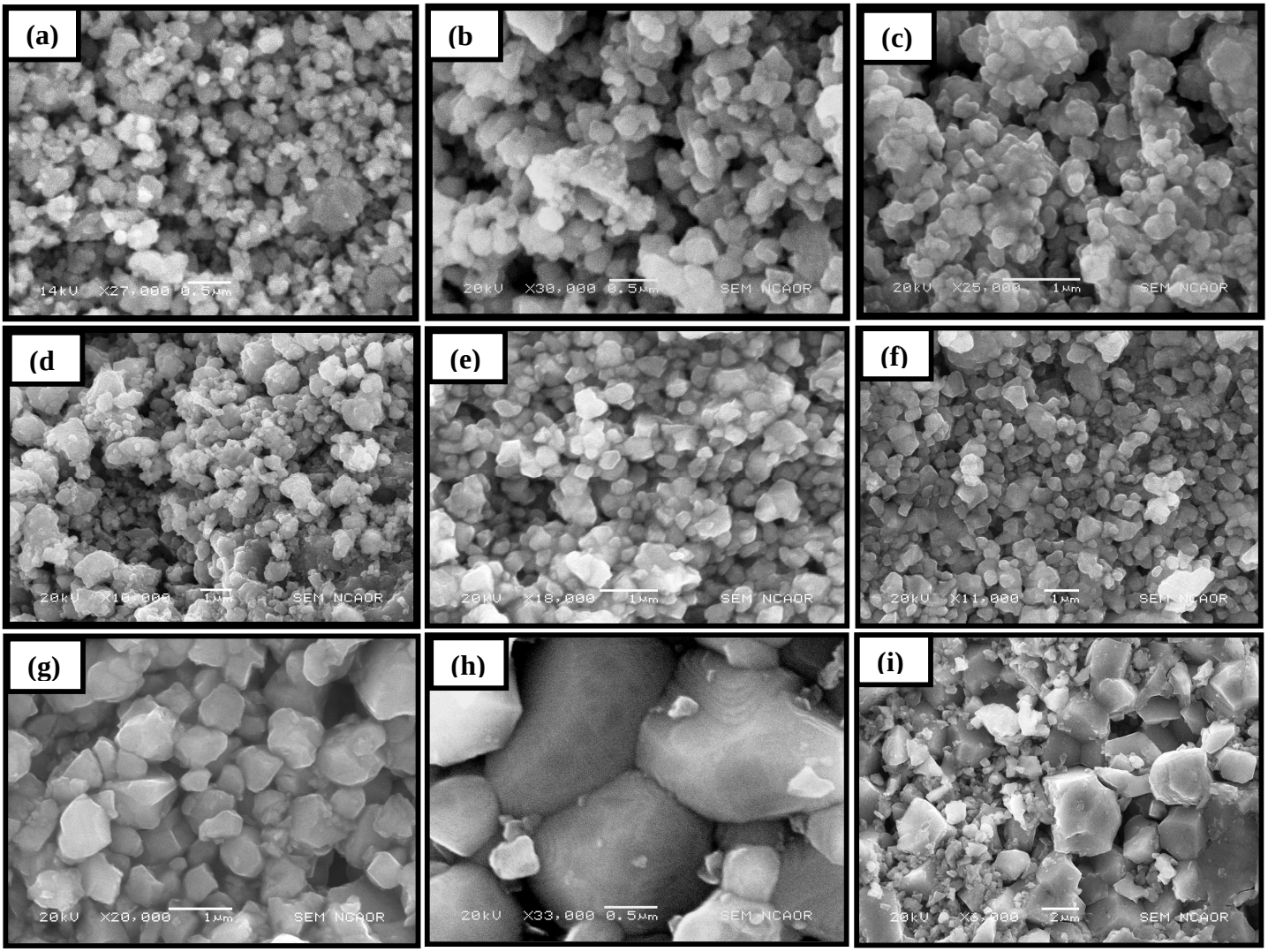

Fig. 6.4. SEM micrographs of $Ni_{1-x}Zn_xFe_2O_4$ showing the change of microstructure with changing value of x and sintering condition (a) x = 0.20, unsintered, (b) x = 0.35, unsintered,(c) x = 0.50, unsintered, (d) x = 0.60, unsintered (e) x = 0.35, sintered at 1100^0C, (f) x = 0.50, sintered at 1100^0C, (g) x = 0.20, sintered at 1200^0C, (h) x = 0.60, sintered at 1200^0C, (i) x = 0.60, sintered at 1300^0C.

For this purpose, four sets of pellets were prepared, (i) one pellet was kept unsintered in order to preserve the nanostructure (ii) the other set of pellets were sintered at 1100, 1200 and 1300^0C for two hours.

The results are summarized as follows:
(i) SEM micrographs of the unsintered samples (Fig. 6.4 (a-d)) revealed uniform, agglomerated and spherical shaped nanopowders of Ni-Zn ferrite.

(ii) When sintering temperature was 1100^0C, the grains grew in size and agglomeration was reduced but porosity could still be seen in the SEM micrographs. (Fig. 6.4 (e-f))

(iii)Sintering at 1200^0C resulted in formation of well-defined bigger grain sizes The samples were characterized by uniform grain growth, homogenous microstructure and average grain size less than 2 μm (Fig. 6.4 (g-h)). Though sintering temperature was reasonably high (1200^0C), Zn loss was not observed in our samples which ensures the maintenance of stoichiometry of the final product. Inhomogeneity or partial precipitation of impurity phase was not observed for our samples whereas in most of the reported results, Zn loss at high temperatures has been observed in SEM micrographs as pore formation within the grains [66-68].

(iv) When sintered was performed at 1300^0C, well-defined microstructure was completely destroyed (Fig. 6.4 (i)).

6.2.5 DC Resistivity measurement:

DC resistivity of the unsintered and sintered pellets was measured from room temperature (27^0C) to 225^0C by using the two-probe method for all values of x and its variation with temperature is shown in Fig. 6.5.

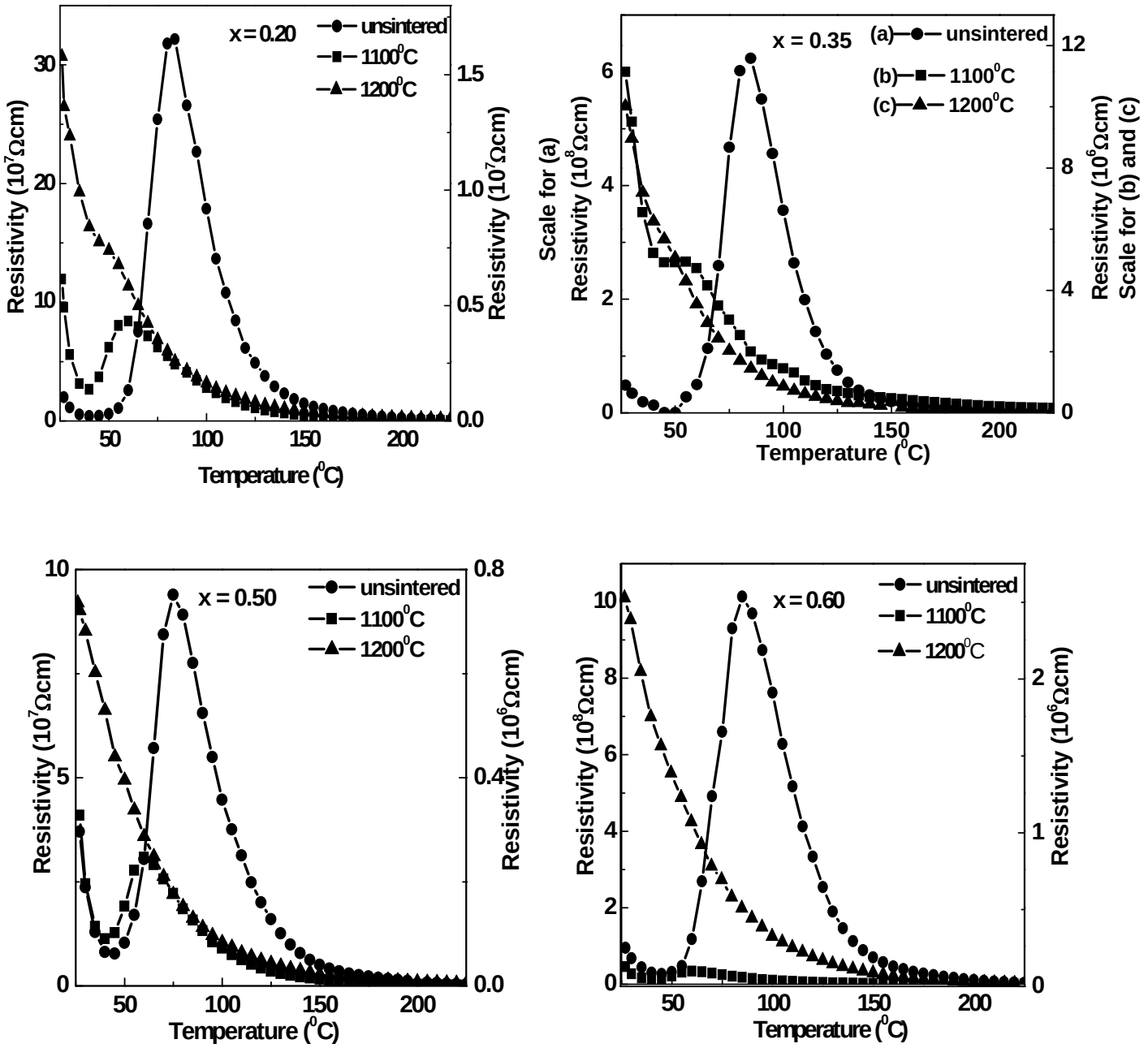

Fig 6.5 DC resistivity for the series of $Ni_{1-x}Zn_xFe_2O_4$ nanopowders with respect to temperature for unsintered samples and samples sintered at 1100 and 1200^{0}C. Left Y axis is the scale for unsintered and sintered samples at 1100^{0}C and right Y axis is the scale for samples sintered at 1200^{0}C for x = 0.20, 0.50 and 0.60 . For x = 0.35, scales are indicated in the figure.

Room temperature resistivity values for the series of composition ($Ni_{1-x}Zn_xFe_2O_4$ with x = 0.20, 0.35, 0.50 and 0.60) sintered at various temperatures are listed in Table 6.2.

Table 6.2. Room temperature (27^0C) DC resistivity of Ni-Zn ferrites for unsintered samples and samples sintered at 1100 and 1200^0C.

Composition $Ni_{1-x}Zn_xFe_2O_4$	DC Resistivity (Ω cm)		
	unsintered	1100^0C	1200^0C
x = 0.20	2.0×10^7	9.6×10^7	1.4×10^7
x = 0.35	4.8×10^7	1.1×10^7	1.0×10^7
x = 0.50	3.7×10^7	4.1×10^7	0.72×10^6
x = 0.60	9.5×10^7	4.5×10^7	2.5×10^6

The impact of microstructure, sintering temperature and composition in the series of $Ni_{1-x}Zn_xFe_2O_4$ ($0 \leq x \leq 1$) powders on the resistivity is discussed below.

(i) Impact of microstructure:

It was observed that the room temperature resistivity of the unsintered samples was of the order of ~ $10^7\Omega$cm. With increase in temperature, the resisitivity increased and a maximum was recorded in the temperature range of ~ 80-100^0C. This behavior might be attributed to the presence of open porosity, loose agglomeration of ultrafine powders and entrapped moisture inside the pores of the powders (humidity recorded in our lab was ~91% at room temperature) [12, 13, 136]. Increasing the temperature up to ~100^0C caused the evaporation of moisture from the samples and therefore, maximum resistivity is attained. This maximum in resistivity

corresponds to desorption of moisture from the samples [12, 13, 123, 126, 131, 135, 136]. Beyond ~100^0C, the samples exhibit typical negative temperature coefficient of resistance (NTCR) behavior of ferrites [38]. Such high resistivities can be explained by simply understanding the fact that smaller grains would offer greater resistance to electron path.

When the samples were sintered at 1100^0C, the grains grew in size and also the porosity was reduced. Therefore, the impact of adsorption of moisture in these samples was also less pronounced especially for x = 0.35. This was indicated by the complete loss of moisture at a temperature lower than ~100^0C (Fig.6.6 (a-d)) for all values of x due to fewer number of pores.
The samples sintered at 1100^0C possessed comparable resistivities to those of as-synthesized nanopowders. This might be due to restricted grain growth. (as seen in SEM micrographs (Fig 6.4 e-f)).

The microstructures of samples sintered at 1200^0C revealed the absence of any intergranular porosity especially for higher Zn concentration (x = 0.60). Therefore, these samples exhibited typical NTCR behavior of ferrites from room temperature to 225^0C.

(ii) Impact of sintering temperature:
Increasing the sintering temperature of the samples from 1100 to 1200^0C resulted in decrease in room temperature resistivity for all the compositions. The reduction in resistivity on increasing the sintering temperature can be attributed to higher amount of densification and bigger grain sizes with lesser number of insulating grain boundaries.

(iii) Impact of Zn content on the series of $Ni_{1-x}Zn_xFe_2O_4$ ($0 < x < 1$) powders:
Zinc is known to promote densification and grain growth in the samples and large grains with lesser number of grain boundaries would cause a decrease in the resistivity [66]. While the nanopowders and samples sintered at 1100^0C seem to be independent of the zinc content in the samples, the samples sintered at 1200^0C exhibit a drop in the resistivity from 10^7 t0 10^5 Ω cm with increase in zinc content.

6.2.6 Magnetization Measurement:

Room temperature saturation magnetization (M_s) and coercivity (H_c) of the as-synthesized nanopowders was measured and the hysteresis loops for all compositions are shown in Fig. 6.6. The measured values for the series of composition $Ni_{1-x}Zn_xFe_2O_4$ ($0 < x < 1$) are listed in Table 6.3.

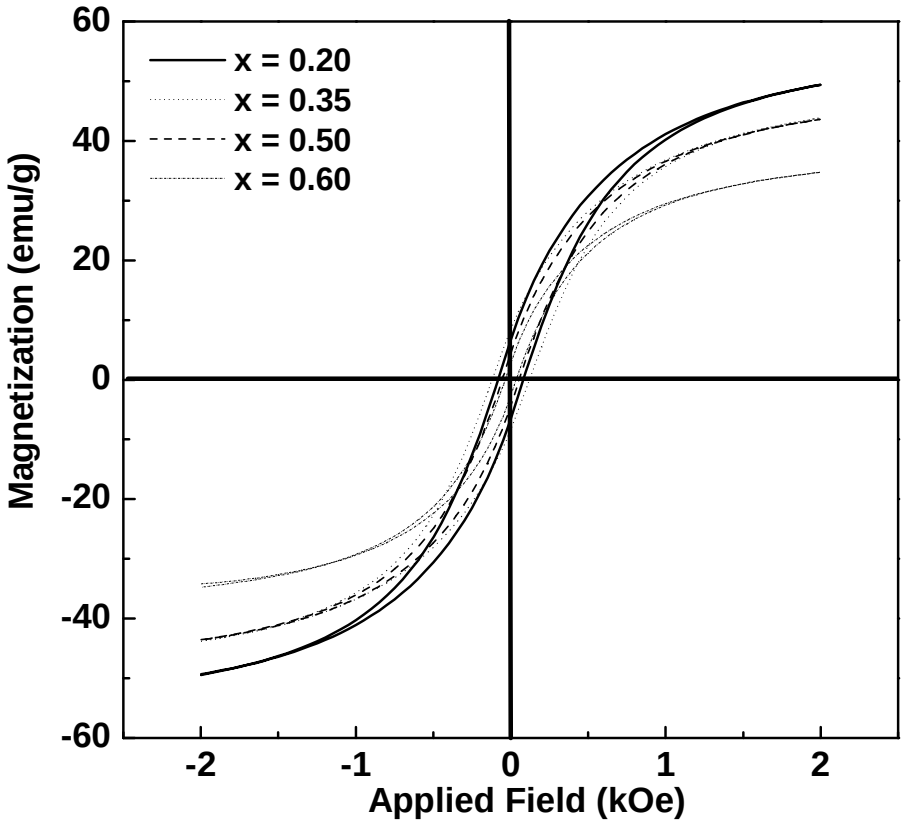

Fig 6.6 Room temperature hysteresis loops for the series of $Ni_{1-x}Zn_xFe_2O_4$ nanopowders.

Table 6.3 Room temperature saturation magnetization and coercivity of different compositions.

$Ni_{1-x}Zn_xFe_2O_4$	M_s (emu/g)	H_c (Oe)
x = 0.20	49.4	81.6
x = 0.35	43.8	120.4
x = 0.50	43.6	55.1
\x = 0.60	34.7	35.0

It was observed that, the saturation magnetization decreased with increasing Zn^{2+} concentration (x= 0.20 - 0.60) from 49.4 to 34.7 emu/g. Zn^{2+} ions have an affinity to occupy tetrahedral (A) sites and Ni^{2+} ions have a tendency to go into the octahedral (B) sites in the crystal lattice, [44] while Fe^{3+} ions are distributed over both the sites. It might happen that as the concentration of diamagnetic Zn^{2+} on A sites is increased, the Fe^{3+} ions were pushed from A to B sites. This decrease in the magnetic ions at A site resulted in a weakened A-B exchange coupling and hence a diminished moment [43, 136].

Discussion:

The oxalate based precursor method for preparation of Ni-Zn nanoferrites has not yet been well explored. Moreover, use of water as the solvent in oxalate precursor based method has been a major challenge till now. Though the oxalate method seems to be very convenient, it is also associated with some problems, such as segregation of impurity phase in the final product. This is due to the less solubility of metal oxalates in pure aqueous medium that quite often precipitate out from the reaction mixture and form small amount of impurity in the form of metal oxides in the final product [81]. The purity of synthesized material is crucial for the accurate measurement of physical properties (such as electrical and magnetic properties). Tailhades et al have reported an

oxalate coprecipitation method for synthesis of ferrites using aqueous alcoholic medium in order to avoid the precipitation of metal oxalates during synthesis [137]. Apart from this, in oxalate co-precipitation method, during filtration and washing of the precipitates, loss of some micro amount of metal ions may occur. This loss may not be detected by XRD but may affect the properties. Therefore, it is vital to determine the appropriate reaction conditions to obtain pure, single phase, nanostructured ferrites by this method.

TG-DTG-DSC, XRD and TEM analyses of the synthesized precursors and calcined powders confirmed that oxidative decomposition of precursor leads to the formation of single phase Ni-Zn ferrite nanopowders. In this chemical method, the reaction of oxalic acid with metal nitrates results in formation of metal oxalate chelate complex. The chelating agent (oxalic acid) is used to keep the metal ions homogenously dispersed in the aqueous solution. Complete dehydration of this solution is accompanied by the partial decomposition of the metal oxalate chelate complex and results in an organic based, voluminous mass, known as "precursor". The thermal decomposition of the precursor causes evolution of CO_2 and NO_x gas and formation of fine particles of Ni-Zn ferrite. The chelate complex nature of the precursor and *in situ* gas evolution during its decomposition prevents the agglomeration of resulting oxide particles and facilitates their nanostructure formation [57, 136].

Generally, the solubility of pure metal oxalate (e.g., iron oxalate, zinc oxalate) complexes is less in aqueous medium. Therefore, they can easily precipitate out from the reaction mixture and eventually form segregated metal oxides and are present as impurity in the final product. But when the amount of oxalic acid is comparatively less (as here), there is a probability of formation of chelate complex by bridging different metal ions where H_2O can also get coordinated with the metal atoms and form a water-soluble complex [138]. Therefore, we can conclude that small amount of oxalic acid (as used here) in the reaction mixture used for preparing the precursor, decreases the probability of preferential precipitation of water insoluble metal oxalates. This results in the formation of pure Ni-Zn ferrite phase at a calcination temperature of 850^0C.

DC resistivity measurements indicated that it was strongly correlated with the sintering condition and the composition and hence the microstructure of the samples. The resistivity of the nanopowders was found to be affected by moisture due to their high porosity and low green density (~2.5-2.8 g/cm^3). However, for the samples sintered at 1100^{0}C, the effect of moisture was less pronounced as sintering results in densification (sintered density~2.8-3.2 g/cm^3) and grain growth. This is especially true for x = 0.35 composition as it exhibited NTCR behavior throughout the measured temperature range (Fig. 6.5). For the samples sintered at an even higher temperature of 1200^{0}C, the effect of moisture was absent (sintered density ~3.4-4.1 g/cm^3) and the samples exhibited the typical NTCR behavior of ferrites.

6.3 Summary of Results:

1. Ni-Zn ferrite nanopowders were successfully synthesized by using oxalate precursor based synthesis route.
2. Major thermal decomposition of the precursor was complete at ~550^{0}C.
3. Single phase Ni-Zn ferrite was formed at a calcination temperature of 850^{0}C for two and a half hours in air atmosphere.
4. Average particle size of nanopowders was ~ 35 nm.
5. Surface morphology studies revealed that the the nanoparticles were round in shape.
6. Room temperature resistivity of as-synthesized nanopowders was ~10^7 Ω cm.
7. Room temperature saturation magnetization varied in the range of 34.7 to 49.4 emu/g and the coercivity varied between 35.0 and 81.6 Oe depending on the composition.